RSC Advances

PAPER

View Article Online
View Journal | View Issue

Cite this: *RSC Adv.*, 2024, **14**, 24196

Utilizing *Chamaerops humilis* in removing methylene blue dye from water: an effective approach

Wassim El Malti, *[a] Saja Koteich[b] and Akram Hijazi[b]

Removing dyes, particularly methylene blue, from wastewater is crucial due to their detrimental effects on environmental and human health. Adsorption, recognized as a simple and efficient technique, is frequently employed to eliminate various dyes from water. Although activated carbon is a favored adsorbent for wastewater treatment, its high cost often restricts its use. As a result, there is increasing interest in utilizing inexpensive, natural materials, and waste products as alternative adsorbents. Sawdust from the European fan palm tree, specifically *Chamaerops humilis*, a widely available and cost-effective by-product, has demonstrated effective dye removal from wastewater. This study explored the impact of various factors such as time, agitation, adsorbent quantity, dye concentration, pH, and temperature on the adsorption of methylene blue using *Chamaerops humilis* sawdust. Optimal dye adsorption conditions were identified at a temperature of 25 °C, a pH of 8, an adsorbent dosage of 100 mg, a contact time of 120 min, and a dye concentration of 20 mg L^{-1}, achieving a removal efficiency of 93.5%. Moreover, the Langmuir isotherm model described the adsorption dynamics more accurately, suggesting a maximum sorption capacity of 22.7 mg g^{-1} for the sawdust. Additionally, adsorption kinetics aligned better with the pseudo-second-order model than the pseudo-first-order model, underscoring the efficacy of this method in treating dye-polluted water.

Received 22nd April 2024
Accepted 29th July 2024

DOI: 10.1039/d4ra02983f

rsc.li/rsc-advances

Introduction

Water is essential for all forms of life, not just humans. Our planet holds about 1380 million cubic kilometers of water, consisting of salty and fresh water. The vast majority, 97.2%, is found in oceans and seas, leaving only 2.8% as freshwater. However, accessible freshwater for human use is just a fraction, about 0.07% of the total, including sources like groundwater, rivers, and lakes. Surprisingly, about 2.15% of this freshwater is locked up in ice.[1]

With industrial growth, more pollutants enter our environment, contaminating the water with dyes, heavy metals, and other harmful substances. Dyes, in particular, are used extensively across various industries, including textiles, plastics, and paper, leading to significant environmental concerns. Even small amounts of dyes, less than 1 part per million in some cases, can be easily seen in water and are not desired due to their impact on the appearance and quality of water bodies.[2] Methylene blue (MB), a common synthetic dye, is especially notorious for its persistence in aquatic environments and potential toxicity to aquatic life, affecting exposed species' reproductive and respiratory systems.[3] Even low concentrations can have detrimental effects, highlighting the urgency for effective removal methods.[4] Dye pollution is characterized by its large volume, intense color, high organic content, and difficulty in breaking down, posing risks to aquatic health and hindering the photosynthesis of waterborne microorganisms.[3]

Several treatment methods, such as adsorption, coagulation, ion exchange, membrane filtration, chemical degradation, and biodegradation, have been explored to combat dye pollution in water.[5] However, many conventional techniques face high costs and operational complexities.[6,7] Chemical degradation methods often involve using hazardous reagents and produce secondary pollution.[7–9] Biodegradation, while environmentally friendly, typically requires long treatment times and specific conditions that can be difficult to maintain.[10–12] In contrast, adsorption offers several advantages, including high efficiency, cost-effectiveness, ease of operation, and the ability to handle a wide range of dye concentrations and types.[6,13–15] These attributes make adsorption a superior method for treating dye-contaminated water compared to physical, chemical, and biological methods.[11] Still, the high cost and regeneration issues of activated carbon, a common adsorbent, limit its widespread use.[16] Recently, research has shifted towards exploring affordable, unconventional adsorbents like clays, agricultural wastes, and industrial by-products.[17–19] Many studies have examined the

[a]*College of Health Sciences, American University of the Middle East, Kuwait. E-mail: Wassim.elmalti@aum.edu.kw*

[b]*Research Platform for Environmental Science (PRASE), Doctoral School of Science and Technology, Lebanon*

removal of dyes from wastewater using a range of adsorbents.[20–24]

Chamaerops humilis, commonly known as the European fan palm, is widely distributed across the Mediterranean region, marking its abundance in diverse environments from coastal areas to mountainous landscapes.[25] Sawdust from *Chamaerops humilis* (SCH), an abundant and low-cost by-product of the palm industry, has emerged as a promising solution for environmental cleanup, particularly in removing heavy metals and dyes from water. Its porous structure and natural composition make it an effective adsorbent, capable of binding with and capturing a wide range of pollutants.[26] Studies have shown that when treated and used in water treatment processes, SCH can significantly reduce concentrations of harmful substances, including heavy metals and synthetic dyes, from contaminated water. This makes it a sustainable option for wastewater treatment and adds value to what is otherwise considered waste material, contributing to a circular economy and reducing reliance on more expensive or non-renewable resources for water purification.[27,28]

This study aimed to assess the effectiveness of valorized SCH in adsorbing MB. We analyzed the chemical and physical characteristics of the adsorbent through various techniques. We conducted batch experiments to evaluate its adsorption capabilities, varying parameters such as particle size, agitation, adsorbent mass, pH, temperature, and contact time. We further examined the kinetics of the adsorption process and developed Langmuir and Freundlich isotherms under optimal conditions to explore its dynamics. The study was concluded with tests on selectivity and reusability of the adsorbent.

Materials and methods

Reagents

All reagents were sourced from commercial suppliers and used as received without additional purification. The used MB is a basic dye (C.I. 52015), presenting as a solid with a maximum absorption wavelength (λ max) of 663 nm and a molar absorptivity (ε) of 170.1 $dm^3\ g^{-1}\ cm^{-1}$. The chemical structure of MB is depicted in Fig. 1. The study also utilized hydrochloric acid (BDH Chemicals, 36.5–38%), sodium hydroxide (Sigma-Aldrich, >97%), and methylene orange (MO), C.I.13025, with a molecular mass of 327.34 g mol^{-1} and a λ_{max} of 464 nm.

Adsorbent preparation

Chamaerops humilis plants were harvested from a region in Lebanon, specifically selecting the petiole part of the plant for processing into SCH (Fig. 2). Approximately 0.5 kg of this sawdust was thoroughly washed multiple times with distilled water to eliminate dust and other impurities. Subsequently, the SCH was oven-dried for 24 hours at 50 °C to achieve complete dryness.

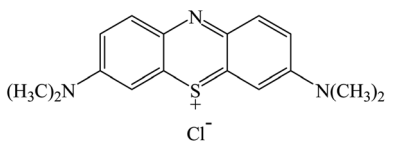

Fig. 1 Structure of MB.

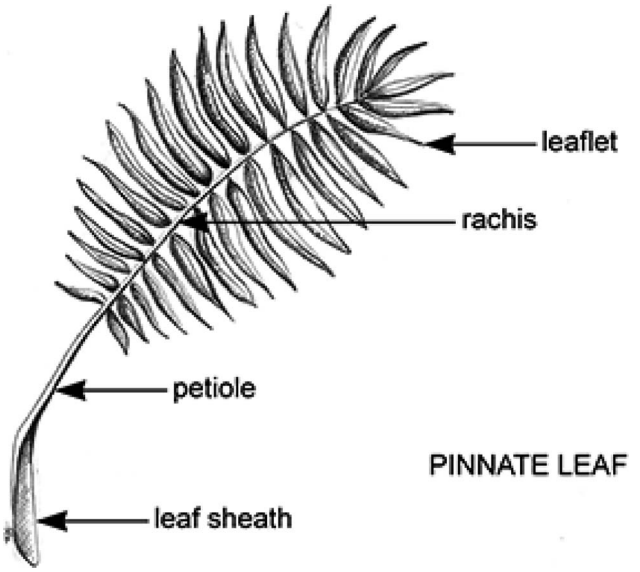

Fig. 2 *Chamaerops humilis* structure.

Techniques and machines

Following the preparation of the SCH, 0.5 kg of the latter was washed multiple times with distilled water, and the total dissolved solids (TDS) in the wash water were monitored to remove the residual salts and investigate the cleanliness of the sawdust.

The moisture content was calculated according to eqn (1) below.

$$\text{Moisture content} = \frac{\text{initial mass} - \text{final mass}}{\text{initial mass}} \times 100 \quad (1)$$

Initial and final masses correspond to the SCH sample before and after drying.

The pH was measured by dispersing 0.5 g of SCH in 50 mL of distilled water, followed by stirring the mixture for 2 h at room temperature.

The pH_{pzc} was determined by adjusting the pH of a 0.01 M NaCl solution to between 2 and 7 using 0.5 M HCl or 0.5 M NaOH. Subsequently, 0.5 g of SCH was added to 20 mL of this pH-adjusted solution and stirred at room temperature for 24 h. The final pH was measured and plotted against the initial pH, with the pH_{pzc} identified where the initial pH (pH_i) equals the final pH (pH_f).

The sample's chemical composition was assessed using energy-dispersive X-ray spectroscopy on a Philips X'pert Pro MPD diffractometer. The Fourier Transform Infrared Spectroscopy (FTIR) analysis was performed using the JASCO FTIR-6300 spectrometer, covering a range from 400 to 4000 cm^{-1}. The BET analysis was conducted on a Micromeritics ASAP 2010; the N_2 adsorption isotherm was obtained by measuring the amount of

N_2 gas adsorbed on the surface of SCH at 77 K, while desorption isotherms were obtained by measuring the amount of gas removed from the surface of SCH as the pressure was gradually reduced. The adsorption was evaluated by ultraviolet-visible spectroscopy (UV-vis; U-2900, dual-beam spectrometer, 200 V, 664 nm wavelength).

Adsorbate preparation

MB stock solution was prepared at a concentration of 1 g L^{-1} by dissolving the dye in distilled water. Desired adsorbate concentrations were then achieved by diluting this stock solution accordingly.

Adsorption tests

Batch mode experimental conditions were assessed using 25 mL Erlenmeyer flasks, wherein a solution of MB (20 mg L^{-1}) was introduced along with 0.025 g of SCH adsorbent. The mixture was agitated at room temperature at medium speed for a predetermined period. Post adsorption, the MB concentration in the solution was analyzed using UV-vis spectroscopy. The study explored the influence of various parameters, including particle size, agitation, adsorbent dose, contact time, pH, and temperature, on the adsorption efficiency. The pH of the adsorptive solutions was adjusted as necessary using HCl and NaOH solutions. The findings from these experiments were utilized to determine the optimal conditions for maximizing MB removal from the aqueous solutions. The percentage of dye removal and the quantity of dye adsorbed were calculated using eqn (2) and eqn (3), respectively.

$$\text{Absorption}\% = \frac{C_0 - C_e}{C_0} \times 100 \quad (2)$$

$$Q_e = \frac{(C_0 - C_e) \times V}{m} \quad (3)$$

C_0 and C_e (mg L^{-1}) represent the initial dye concentration and equilibrium concentration, respectively. V is the volume of the solution (L), and m is the adsorbent mass (g).

Adsorption isotherm models

Langmuir. Assuming a uniform adsorbent surface with a monolayer formation, the adsorption is presumed to follow the same mechanism without any interaction among the adsorbed molecules. The Langmuir isotherm can be represented by the linear eqn (4):[20,29,30]

$$\frac{C_e}{Q_e} = \frac{1}{Q_m \times K_L} + \frac{C_e}{Q_m} \quad (4)$$

C_e represents the MB concentration at equilibrium (mg L^{-1}), Q_e is the adsorption capacity at equilibrium (mg g^{-1}), Q_m is the maximum adsorption capacity for a monolayer (mg g^{-1}), and K_L is the Langmuir constant associated with adsorption energy (L g^{-1}).

Subsequently, the separation factor constant (R_L) derived from the Langmuir model is calculated using eqn (5):[20,29,30]

$$R_L = \frac{1}{1 + K_L C_0} \quad (5)$$

C_0 is the initial concentration of MB (mg L^{-1}).

Freundlich. This model assumes adsorption forms multilayers on a heterogeneous surface. The Freundlich linear eqn (6) is given by:[20,29,31]

$$\log Q_e = \log K_F + \frac{1}{n_F} \log C_e \quad (6)$$

Q_e is the equilibrium adsorption capacity (mg g^{-1}), C_e is the equilibrium MB concentration (mg L^{-1}), K_F is the Freundlich constant related to adsorption capacity, and n_F is the Freundlich exponent indicating adsorption intensity.

Reusability tests

These tests were conducted on dried samples of SCH, which had previously been loaded with MB under optimal conditions. Each sample was placed in a 150 mL Erlenmeyer flask containing 100 mL of 90% ethanol and stirred at 25 °C for 2 h. After desorption, the MB-laden solution was analyzed using UV-vis spectroscopy. This adsorption and desorption cycle was repeated four times, resulting in five uses for each adsorbent.

All the experiments in this study were performed in triplicate, exhibiting a standard deviation of 1.5% and a reproducibility of 0.4%.

Results and discussion

Enhancing the adsorbent performance: the impact of washing frequency

Fig. 3 illustrates the TDS values in the wash water as the sawdust underwent successive washes. We observed a decline in water TDS from 200 to 11 ppm, indicating a reduction in residual salts. The TDS stabilized at 11 ppm after the eighth wash, suggesting no further washing was necessary as the sawdust

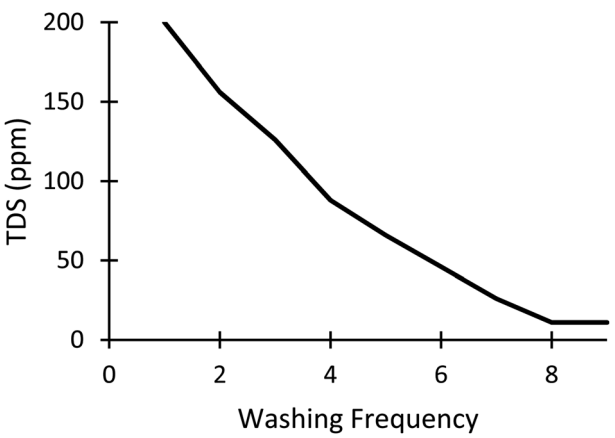

Fig. 3 TDS variation *vs.* number of washings with distilled water.

had become sufficiently clean. Notably, a TDS level of 11 ppm is considered suitable and acceptable for adsorption.[32,33]

Physico-chemical properties of the adsorbent

Table 1 shows that the adsorbent derived from *Chamaerops humilis* sawdust exhibited notable characteristics essential for its application in water purification processes. The moisture content stood at 9.80%, reflecting a good-quality adsorbent.[21,34] The pH value of the adsorbent was slightly acidic at 6.5, with the point of zero charge (pH_{zpc}) being close at 6.0, suggesting a balanced surface charge distribution under neutral conditions. The chemical analysis revealed a composition rich in carbon, highlighting its potential for adsorption, and a rich composition in oxygen, indicating various oxygen-containing functional groups. The surface properties of SCH, including specific surface area, total pore volume, and average pore size were measured using N_2 adsorption–desorption isotherms (Table 1). The results revealed that the SCH has a porous structure, with a relatively small BET surface area of 12.50 $m^2 g^{-1}$ and an average pore diameter of 2.500 nm. According to the International Union of Pure and Applied Chemistry (IUPAC) classification on pore dimensions, adsorbent pores are categorized as micropores (d < 2 nm), mesopores (d = 2–50 nm), and macropores (d > 50 nm). Therefore, with an average pore diameter of 2.500 nm, the majority of the SCH pores fall into the mesoporous range.

The FTIR analysis (Fig. 4) confirmed the presence of many functional groups, with broad bands observed for O–H stretching (3220–3450 cm^{-1}), indicative of the high presence of carboxyls, phenols, and alcohols groups; one absorption peak at about 1557.00 cm^{-1}, characteristic of the C=O stretching of the carbonyl groups; the C–H stretching vibrations at 2942.30 cm^{-1}, and C–O stretching at 1048.20 cm^{-1}, can be attributed to the alcohol, phenol, and ether groups. These properties collectively underscore the adsorbent's potential for effectively interacting and removing MB from water.

Table 1 Physico-chemical properties of SCH

Moisture content (%)		9.8
pH		6.5
pH_{zpc}		6.0
Chemical composition (wt%)	C	58.48
	H	5.580
	N	1.420
	O	34.36
Total surface area ($m^2 g^{-1}$)		12.5
Total pore volume ($cm^3 g^{-1}$)		0.725
Average pore size (nm)		2.5

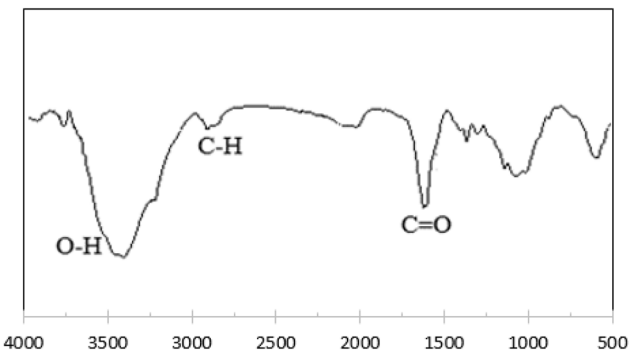

Fig. 4 FTIR analysis of SCH.

Adsorption tests

Several variables can influence the efficiency of MB adsorption using SCH. Extensive investigation has been conducted to explore the effect of these variables on the adsorption process. For optimal adsorption results, it's crucial to fine-tune these conditions during laboratory experiments.

Effect of particle size. To demonstrate how particle size influences the adsorption of MB on SCH, an investigation was conducted using two particle size ranges: 0.16–0.40 mm and 0.41–1.0 mm. The conditions were constant: temperature at 25 °C, MB concentration at 20 mg L^{-1}, adsorbent dosage at 25 mg, and contact time at 120 min. Fig. 5 shows that smaller adsorbent particles achieved higher adsorption efficiency, with around 72% adsorption for the 0.16–0.4.0 mm range, compared to 50% for the 0.4–1.0 mm range. This difference is likely due to smaller particles providing a larger surface area, enhancing the adsorbate's access to the adsorbent's pores. Since sorption is primarily a surface-based process, a smaller particle size means a larger available surface area, leading to increased sorption at equilibrium.[35]

Effect of agitation. Agitation helps distribute dye molecules throughout the solution and affects the formation of the external boundary film.[36] In our study, we compared adsorption under stationary conditions and with agitation while maintaining other variables constant at a temperature of 25 °C, MB concentration of 20 mg L^{-1}, adsorbent dose of 25 mg, and a contact time of 120 min. Fig. 6 illustrates that the adsorption efficiency was 44% higher with agitation compared to the stationary condition. This increase can be attributed to the enhanced adsorbate–adsorbent interaction.

Effect of adsorbent mass. The amount of adsorbent used, or the adsorbent dose, is crucial in adsorption experiments as it impacts how much dye can be removed from a solution. In our

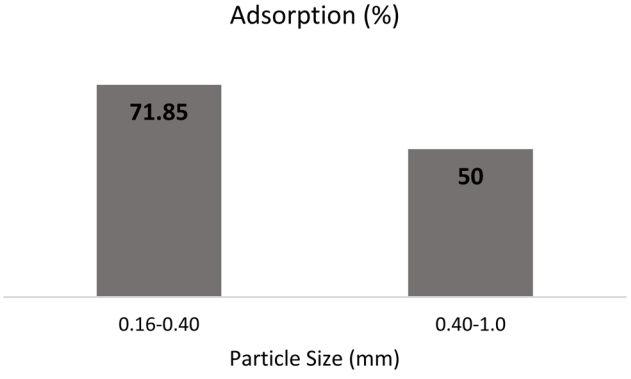

Fig. 5 Effect of SCH particle size on the MB adsorption (%).

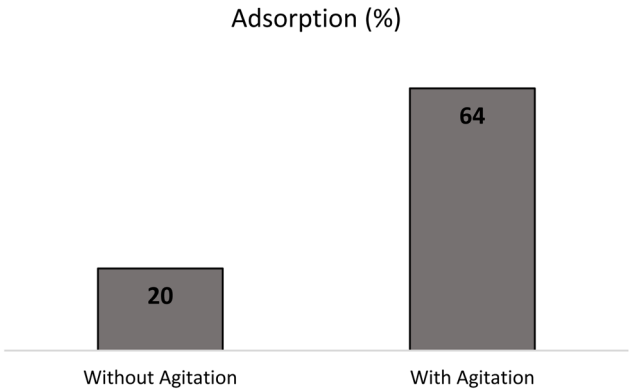

Fig. 6 Effect of agitation on the MB adsorption (%).

tests, we investigated adsorbent doses ranging from 25 to 200 mg at 25 °C for 120 min. The MB concentration was adjusted to 20 mg L^{-1}. According to the data in Fig. 7, increasing the sawdust dose from 25 mg to 150 mg gradually improved the dye adsorption from 60% to a peak of 91%. This improvement is likely due to the larger surface area and more active sites available for adsorption at higher doses. Even though the dye removal slightly increased to 92% and 94% at 175 mg and 200 mg, we identified 100 mg as the optimal dose. This is because using a significantly larger dose may lead to wastage and depletion of adsorbent resources, particularly when scaling up for practical applications.

Effect of pH. The pH level is crucial in dye adsorption onto adsorbents, impacting the surface binding sites' behavior. In this study, we examined how varying pH levels from 2 to 10 affect MB adsorption onto SCH, keeping other conditions like temperature at 25 °C, MB concentration at 20 mg L^{-1}, SCH mass at 100 mg, and contact time at 120 min constant.

The results, depicted in Fig. 8, show the correlation between the pH and MB adsorption on sawdust, where an increase in pH from 2 to 10 leads to an increase in adsorption percentage from 45% to 93%. Specifically, there's a sharp increase in adsorption

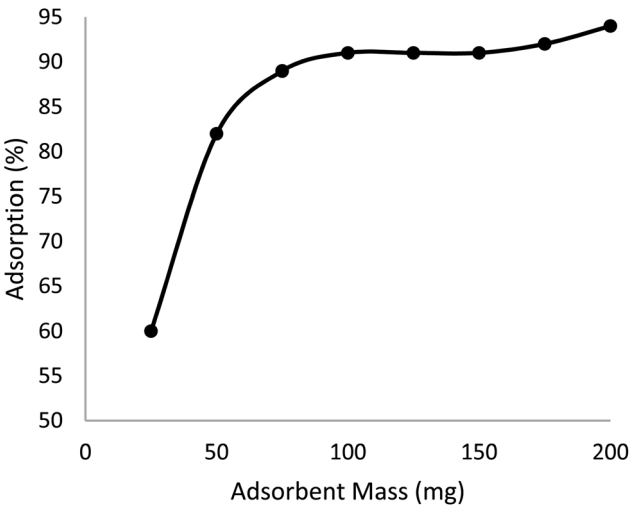

Fig. 7 Effect of SCH mass on the MB adsorption (%).

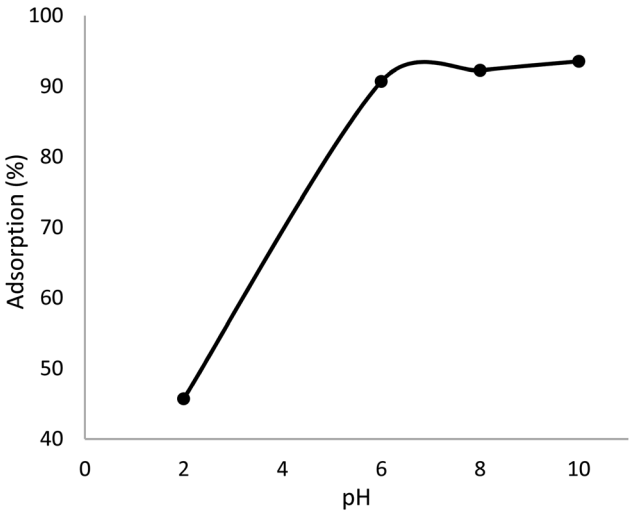

Fig. 8 Effect of the initial pH on the MB adsorption (%).

from 45% to 90% as the pH rises from 2 to 6, followed by a more gradual increase to 93% as the pH goes from 6 to 10. At pH values below 6, the sawdust surface is positively charged, causing repulsive interactions with MB cations and a high concentration of H^+ ions in the solution, which competes with MB for adsorption sites, reducing the removal rate. As the pH increases, the sawdust surface turns negatively charged, enhancing its interaction with the MB molecules.

Based on these observations, we determined that the optimal pH for our experiments is 8 to avoid conditions that are too basic and not representative of urban wastewater characteristics.

Effect of temperature. Temperature significantly influences the adsorption process, with thermodynamic factors like heat of adsorption and activation energy—both temperature-dependent—playing key roles in adsorption dynamics.[37] We examined how varying temperatures (25 to 45 °C) affect adsorption, maintaining conditions such as MB concentration at 20 mg L^{-1}, SCH mass at 100 mg, pH at 8, and a 120 min contact time. Our findings reveal that the adsorption efficiency decreases from 94% to 90% as temperature increases from 25 °C to 45 °C (Fig. 9), indicative of an exothermic process. This decrease in efficiency at higher temperatures could be due to enhanced diffusion rates of the dye across the porous adsorbent's boundary layers, making more active sites accessible for sorption. This observation aligns with other studies where decreased adsorption efficiency with rising temperature was noted, attributed to diminished adsorbent activity.[38] Consequently, we determined that the optimal temperature for maximal MB adsorption using SCH is 25 °C, highlighting that lower temperatures are preferable for the investigated adsorption process.

Effect of contact time. The equilibrium time is an essential parameter in analyzing the adsorption process. We investigated how varying contact times, from 10 to 150 min, impacted the efficiency of MB removal. This relationship is depicted in Fig. 10, showing an increase in adsorption percentage from

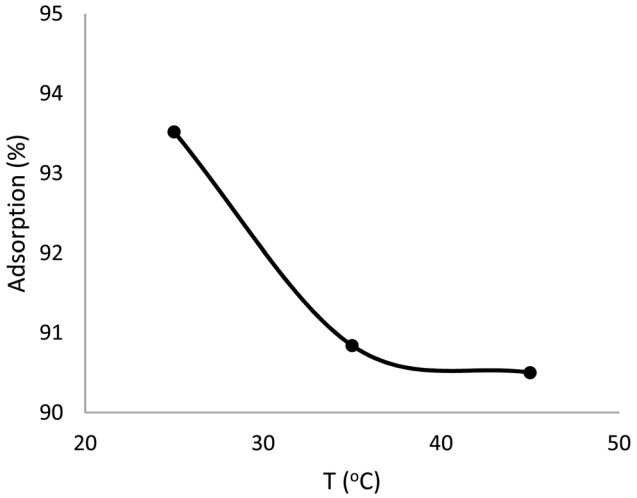

Fig. 9 Effect of temperature on the MB adsorption (%).

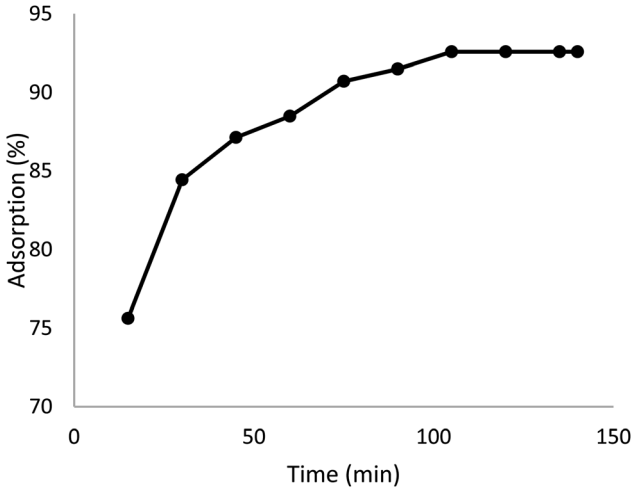

Fig. 10 Effect of contact time on the MB adsorption (%).

75.0% to 92.7% as the contact time extended from 15 to 120 min, with the peak removal efficiency of 92.7% occurring at 105 min.

During the adsorption process, we observed three distinct phases. Initially, the removal of MB was rapid due to the abundance of free active sites on the SCH, allowing a significant amount of MB to bind quickly, which was attributed to the sample surface area and availability of active sites. Following this rapid phase, the adsorption rate decreases as the number of available active sites diminishes. Finally, the process stabilizes, reaching an equilibrium where no further MB is removed from the water, indicating the saturation phase. This slowdown is primarily due to the diminishing number of available active sites on the adsorbent as they become occupied over time.[20]

Adsorption kinetics

In this study, we applied both pseudo-first-order and pseudo-second-order kinetic models to pinpoint the most accurate description of the adsorption of MB onto SCH (eqn (7) and (8)).[39–41] The rate constants for these models, K_1 and K_2, along with the calculated adsorption capacities (Q_e), were derived from the plots of $\ln(Q_e - Q_t)$ *versus* time for the pseudo-first-order model, and t/Q_t *versus* time for the pseudo-second-order model.

$$\ln(Q_e - Q_t) = \ln Q_e - K_1 t \quad (7)$$

$$\frac{t}{Q_t} = \frac{1}{K_2 Q_e^2} + \frac{t}{Q_e} \quad (8)$$

Table 2 presents the values of K_1 and K_2, the correlation coefficients (R^2), and the calculated adsorption capacities (Q_e). Fig. 11a and b visually represent the kinetic plots for the pseudo-first and second-order models, respectively.

The pseudo-first-order model yielded an adsorption capacity ($Q_{e\cdot cal}$) of 2.35 mg g^{-1} for SCH, significantly differing from the experimental data ($Q_{e\cdot exp}$). This discrepancy suggests that the pseudo-first-order model does not adequately capture the adsorption kinetics for our system. Conversely, the pseudo-second-order model's $Q_{e\cdot cal}$ value of 4.80 mg g^{-1} aligns more closely with the experimental value of 4.65 mg g^{-1}. Furthermore, the pseudo-second-order model's correlation coefficient ($R^2 = 0.999$) is substantially higher than that of the pseudo-first-order model ($R^2 = 0.952$), strongly indicating the pseudo-second-order model as the more accurate representation of the kinetics of MB adsorption onto SCH, which underscores the significance of chemisorption. This provides valuable insights into the nature of the adsorption process, suggesting that the interactions are not simply physical but involve chemical bonding between the MB molecules and the active sites on the SCH surface, leading to a more efficient adsorption system.[42] In addition, the better fit of the pseudo-second-order model suggests that the adsorption capacity is closely related to the number of active sites available on the adsorbent.[43] As the model assumes that the adsorption rate is proportional to the square of the number of unoccupied sites, it implies that the adsorption process becomes slower as these sites become occupied, characteristic of chemisorption processes where the active sites play a crucial role.[44]

Table 2 Pseudo-first-order and pseudo-second-order models for the adsorption of MB onto SCH

Kinetic models	Adsorbent (SCH)
$Q_{e\cdot exp}$ (mg g^{-1})	4.65
Pseudo-first order	
$Q_{e\cdot cal}$ (mg g^{-1})	2.35
K_1	0.04
R^2	0.952
Pseudo-second order	
$Q_{e\cdot cal}$ (mg g^{-1})	4.80
K_2	0.05
R^2	0.999

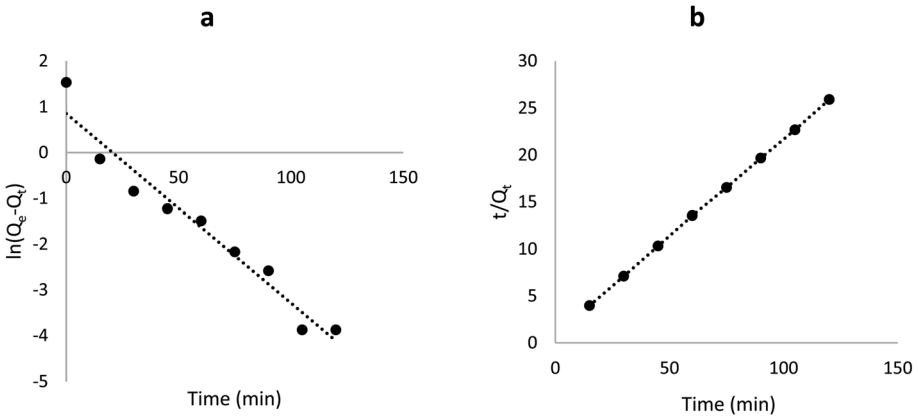

Fig. 11 (a) Pseudo-first-order model; (b) pseudo-second-order models of the adsorption of MB onto SCH.

Adsorption isotherm models

We conducted adsorption isothermal studies to understand how MB interacts with SCH in water and determine the maximum adsorption capacity (Q_e). For this purpose, we applied both the Langmuir and Freundlich isotherm models.

The summary of our isotherm analysis is shown in Fig. 12 and detailed in Table 3. The sawdust was compatible with the Langmuir and Freundlich models for removing MB, as indicated by the plots' strong correlation coefficients and linearity.

The dimensionless separation factor or equilibrium parameter, R_L, is a crucial Langmuir model feature that predicts adsorption viability. An R_L value greater than 1 indicates unfavorable adsorption, zero suggests irreversible adsorption, one denotes linear adsorption, and values between zero and one reflect favorable adsorption.[29] As displayed in Table 3, our findings reveal that the R_L values are within the 0 to 1 range, suggesting that the MB adsorption onto SCH is favorable.

Regarding the Freundlich model, the heterogeneity factor 'n' helps classify the adsorption process: 1 points to linear adsorption, less than 1 to chemical adsorption, and greater than 1 to physical adsorption (physisorption).[29,45] For our study, 'n' values were approximately 3 for the MB adsorption onto sawdust, indicating a physical adsorption process.

Comparing the two models, the Langmuir isotherm provided higher correlation coefficients for the MB sorption, suggesting that the Langmuir model more accurately describes the sorption of MB onto SCH in our study.[29]

By comparing the maximum adsorption capacity of SCH with other materials (natural, synthetic, or treated) reported in the

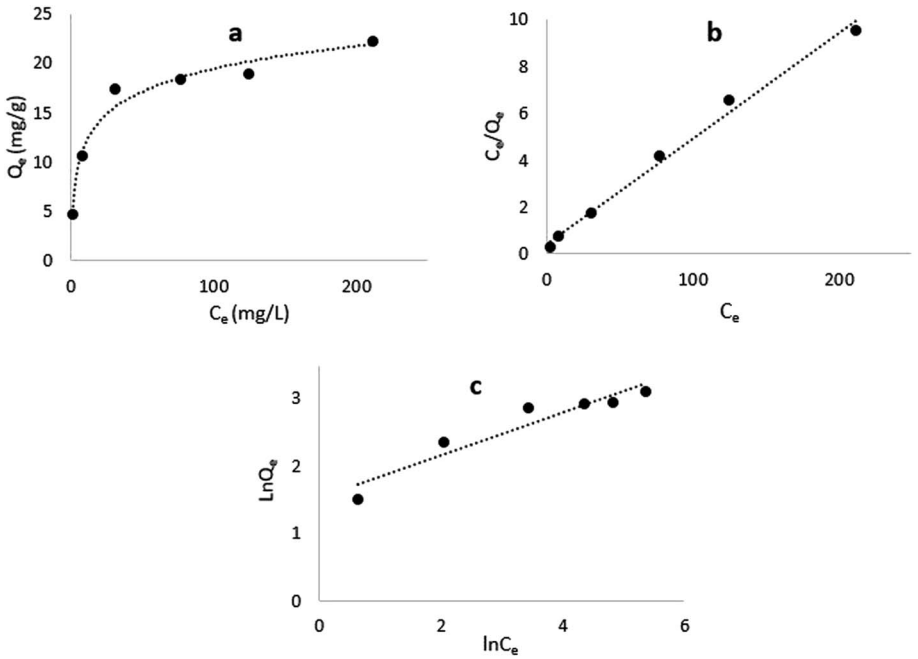

Fig. 12 (a) Adsorption capacity (Q_e) *vs.* several initial concentrations of MB; (b) and (c) Langmuir and Freundlich isotherm plots for the adsorption of MB onto SCH.

Table 3 Langmuir and Freundlich isotherm models data

Adsorption isotherm models	Parameters	Adsorbent (SCH)
Langmuir	Q_m (mg g^{-1})	22.27
	K_L	0.022
	R_L	0.680
	R^2	0.990
Freundlich	K_F	4.620
	n	3.000
	R^2	0.904

literature (Table 4), it is evident that SCH is an effective adsorbent for removing MB from water under mild conditions. This effectiveness is particularly notable given that SCH is a natural and abundant material that is used without any specific treatment.

Selectivity tests

In wastewater, dyes are never present in isolation; they coexist with other dyes. A study was conducted to evaluate the selectivity of SCH in removing cationic MB and anionic dye methyl orange (MO). For this purpose, an aqueous solution containing both dyes at equal concentrations (20 ppm) was prepared at room temperature and a pH of 8. The extent of dye removal was measured using UV-vis spectroscopy. The results, depicted in Fig. 13, indicate that the adsorption efficiency for MB (90%) surpasses that of MO. This disparity can be attributed to the strong interactions between the positively charged MB and the sawdust. Conversely, the MO molecules, being anionic, repel electrostatically against the sawdust, leading to suboptimal adsorption efficiency.

Reusability tests

The employment of adsorption for wastewater treatment presents a considerable benefit over conventional methods due to the potential for adsorbent regeneration. Although SCH adsorbent is a low-cost material readily available in large quantities, particularly in the Mediterranean region, its regeneration was evaluated by exposing it to ethanol as an eluent for up to five reuse cycles at optimal conditions. As shown in Fig. 14, the SCH adsorbent maintain substantial usability for up to three cycles. However, a notable decline in adsorption capacity was observed from the fourth cycle onward, with

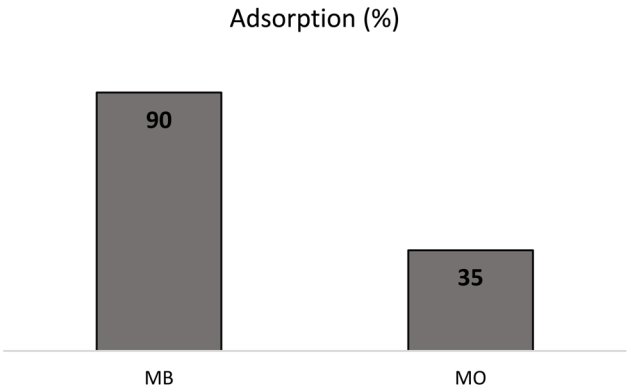

Fig. 13 MB and MO adsorption (%) onto SCH.

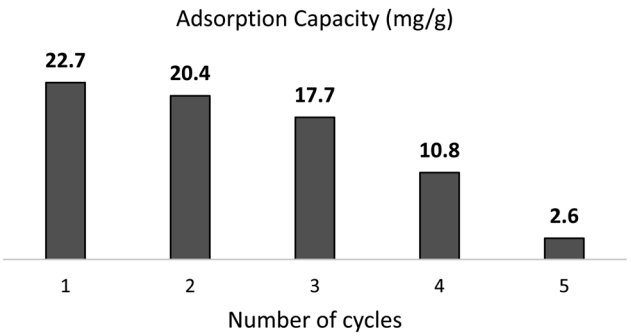

Fig. 14 Plots of adsorption capacity *versus* no. of uses of SCH at optimal conditions.

Table 4 Comparison between the maximum adsorption capacities of SCH and various materials from the literature

Adsorbent	Q_m (mg g^{-1})	Conditions	Year
Banana peels[46]	20.80	30 °C, pH 6–7	2002
Orange peels[46]	18.60	30 °C, pH 6–7	2002
Neem leaf[47]	8.760	27 °C, pH 5–8	2005
Fly ash[48]	13.42	30 °C, pH 10	2005
Eggshell[49]	0.8000	25 °C, pH 7	2006
Wheat shells[50]	16.56	30 °C, pH 4.5–9	2006
Durian skin[51]	7.230	130 °C, pH 9	2015
Haloxylon recurvum plant stems[52]	22.93	25 °C, pH 8	2017
Ficcus palmata[53]	6.890	45 °C, pH 7	2019
Modified (treated) fly ash[54]	28.65	25 °C, pH 7	2021
Activated carbon from grape wood wastes[55]	5.880	25 °C, pH 11	2021
Citrullus colocynthis peels	4.480	19 °C, pH 8	2021
Tumeric/polyvinyl alcohol/carboxymethyl cellulose[56]	6.270	25 °C, pH 6	2022
Reused SiO_2 desiccant + treated sand[57]	22.80	25 °C, pH 7	2023
Cedrus atlantica sawdust[58]	7.840	25–60 °C, pH 10	2023
SCH (this study)	22.70	25 °C, pH 7	2024

a reduction of approximately 50% of its initial maximum capacity. This may be attributed to the partial depletion of adsorption sites after reuse or incomplete desorption of methylene blue.

Conclusions

In this study, valorized sawdust from *Chamaerops humilis*, a low-cost precursor, has been examined and proven to be an efficient adsorbent for removing methylene blue from aqueous solutions. Given that SCH is relatively inexpensive, freely accessible, and abundant, it is a viable low-cost alternative for dye removal from aqueous solutions. This study investigated the impact of various parameters on adsorption efficiency, revealing that increasing the initial pH, adsorbent dose, and contact time enhanced the MB adsorption efficiency, whereas an increase in temperature reduced it. Agitation was shown to be crucial to improving the adsorption process. Furthermore, the pseudo-second-order model was found to more accurately describe the kinetic behavior of MB adsorption compared to the pseudo-first-order model. The values of the determined parameters (n and R_L) using isothermal models indicated that the adsorption process was desirable and predominantly physical. Additionally, the correlation coefficient (R^2) obtained using the Langmuir isotherm model showed a better fit than the Freundlich isotherm model.

Similarly to most of the adsorption studies for wastewater treatment, the efforts exerted in this research study remain confined to the lab-scale. However, for practical industrial-scale applications, effluent treatment should be conducted in a continuous mode.

Data availability

All data generated or analyzed during this study are included in this article.

Author contributions

Conceptualization, formal analysis, methodology, and supervision: WEM, AH; investigation and validation: SK and WEM; funding acquisition and project administration: AH; writing and editing: WEM.

Conflicts of interest

There are no conflicts to declare.

References

1 V. Renaudin, Le dessalement de l'eau de mer et des eaux saumâtres, https://culturesciences.chimie.ens.fr/thematiques/chimie-physique/thermodynamique-chimique/le-dessalement-de-l-eau-de-mer-et-des-eaux, accessed 15 April 2024.
2 R. Al-Tohamy, S. S. Ali, F. Li, K. M. Okasha, Y. A.-G. Mahmoud, T. Elsamahy, H. Jiao, Y. Fu and J. Sun, A critical review on the treatment of dye-containing wastewater: Ecotoxicological and health concerns of textile dyes and possible remediation approaches for environmental safety, *Ecotoxicol. Environ. Saf.*, 2022, **231**, 113160.
3 P. O. Oladoye, T. O. Ajiboye, E. O. Omotola and O. J. Oyewola, Methylene blue dye: Toxicity and potential elimination technology from wastewater, *Results Eng.*, 2022, **16**, 100678.
4 R. Pourbaba, A. Abdulkhani, A. Rashidi and A. Ashori, Lignin nanoparticles as a highly efficient adsorbent for the removal of methylene blue from aqueous media, *Sci. Rep.*, 2024, **14**, 9039.
5 M. Shabir, M. Yasin, M. Hussain, I. Shafiq, P. Akhter, A.-S. Nizami, B.-H. Jeon and Y.-K. Park, A review on recent advances in the treatment of dye-polluted wastewater, *J. Ind. Eng. Chem.*, 2022, **112**, 1–19.
6 G. Crini, Non-conventional low-cost adsorbents for dye removal: A review, *Bioresour. Technol.*, 2006, **97**, 1061–1085.
7 V. K. Gupta, I. Ali, T. A. Saleh, A. Nayak and S. Agarwal, Chemical treatment technologies for wastewater recycling—an overview, *RSC Adv.*, 2012, **2**, 6380–6388.
8 I. Sirés and E. Brillas, Remediation of water pollution caused by pharmaceutical residues based on electrochemical separation and degradation technologies: A review, *Environ. Int.*, 2012, **40**, 212–229.
9 U. G. Akpan and B. H. Hameed, Parameters affecting the photocatalytic degradation of dyes using TiO2-based photocatalysts: A review, *J. Hazard. Mater.*, 2009, **170**, 520–529.
10 H. Ali, Biodegradation of Synthetic Dyes—A Review, *Water, Air, Soil Pollut.*, 2010, **213**, 251–273.
11 E. Forgacs, T. Cserháti and G. Oros, Removal of synthetic dyes from wastewaters: a review, *Environ. Int.*, 2004, **30**, 953–971.
12 R. G. Saratale, G. D. Saratale, D. C. Kalyani, J. S. Chang and S. P. Govindwar, Enhanced decolorization and biodegradation of textile azo dye Scarlet R by using developed microbial consortium-GR, *Bioresour. Technol.*, 2009, **100**, 2493–2500.
13 Y. C. Wong, Y. S. Szeto, W. H. Cheung and G. McKay, Adsorption of acid dyes on chitosan—equilibrium isotherm analyses, *Process Biochem.*, 2004, **39**, 695–704.
14 V. K. Gupta, Suhas, Application of low-cost adsorbents for dye removal – A review, *J. Environ. Manage.*, 2009, **90**, 2313–2342.
15 T. Robinson, G. McMullan, R. Marchant and P. Nigam, Remediation of dyes in textile effluent: a critical review on current treatment technologies with a proposed alternative, *Bioresour. Technol.*, 2001, **77**, 247–255.
16 I. A. W. Tan, A. L. Ahmad and B. H. Hameed, Adsorption of basic dye on high-surface-area activated carbon prepared from coconut husk: Equilibrium, kinetic and thermodynamic studies, *J. Hazard. Mater.*, 2008, **154**, 337–346.
17 S. Kainth, P. Sharma and O. P. Pandey, Green sorbents from agricultural wastes: A review of sustainable adsorption materials, *Appl. Surf. Sci. Adv.*, 2024, **19**, 100562.

18 M. M. Kwikima, S. Mateso and Y. Chebude, Potentials of agricultural wastes as the ultimate alternative adsorbent for cadmium removal from wastewater. A review, *Sci. Afr.*, 2021, **13**, e00934.
19 S. Khan, S. Ajmal, T. Hussain and M. U. Rahman, Clay-based materials for enhanced water treatment: adsorption mechanisms, challenges, and future directions, *J.Umm Al-Qura Univ. Appll. Sci.*, 2023, DOI: **10.1007/s43994-023-00083-0**.
20 W. El Malti, A. Hijazi, Z. A. Khalil, Z. Yaghi, M. K. Medlej and M. Reda, Comparative study of the elimination of copper, cadmium, and methylene blue from water by adsorption on the citrus Sinensis peel and its activated carbon, *RSC Adv.*, 2022, **12**, 10186–10197.
21 W. Al-Khatib, M. Srour, H. Bazzi, C. Haidar, A. Hijazi, A. E.-A. Al-Rekaby and W. El Malti, Test of elimination of cadmium and lead ions from water using polyurethane loaded with Cymbopogon citratus activated carbon, *Biorem. J.*, 2023, **27**, 301–310.
22 M. Rafatullah, O. Sulaiman, R. Hashim and A. Ahmad, Adsorption of methylene blue on low-cost adsorbents: A review, *J. Hazard. Mater.*, 2010, **177**, 70–80.
23 M. T. Yagub, T. K. Sen, S. Afroze and H. M. Ang, Dye and its removal from aqueous solution by adsorption: A review, *Adv. Colloid Interface Sci.*, 2014, **209**, 172–184.
24 M. A. M. Salleh, D. K. Mahmoud, W. A. W. A. Karim and A. Idris, Cationic and anionic dye adsorption by agricultural solid wastes: A comprehensive review, *Desalination*, 2011, **280**, 1–13.
25 A. Giovino, S. Scibetta, S. Saia and C. Guarino, Genetic and morphologic diversity of European fan palm (Chamaerops humilis L.) populations from different environments from Sicily, *Bot. J. Linn. Soc.*, 2014, **176**, 66–81.
26 R. Chikri, N. Elhadiri, M. Benchanaa and Y. El maguana, Efficiency of Sawdust as Low-Cost Adsorbent for Dyes Removal, *J. Chem.*, 2020, **2020**, 8813420.
27 E. Meez, A. Rahdar and G. Z. Kyzas, Sawdust for the Removal of Heavy Metals from Water: A Review, *Molecules*, 2021, **26**(14), 4318.
28 M. N. Sahmoune and A. R. Yeddou, Potential of sawdust materials for the removal of dyes and heavy metals: examination of isotherms and kinetics, *Desalination Water Treat.*, 2016, **57**, 24019–24034.
29 T. F. Akinhanmi, E. A. Ofudje, A. I. Adeogun, P. Aina and I. M. Joseph, Orange peel as low-cost adsorbent in the elimination of Cd(II) ion: kinetics, isotherm, thermodynamic and optimization evaluations, *J. Bioresour. Bioprod.*, 2020, **7**, 34.
30 I. Langmuir, The adsorption of gases on plane surfaces of glass, mica and platinum, *J. Am. Chem. Soc.*, 1918, **40**, 1361–1403.
31 H. Freundlich, Uber die adsorption in losungen, *Int. J. Res. Phys. Chem. Chem. Phys.*, 1906, **57**, 385–470.
32 S. S. M. Hassan, H. I. Abdel-Shafy and M. S. M. Mansour, Removal of pyrene and benzo(a)pyrene micropollutant from water via adsorption by green synthesized iron oxide nanoparticles, *Adv. Nat. Sci.: Nanosci. Nanotechnol.*, 2018, **9**, 015006.
33 P. Beaulieu and B. Fisset, Eau du robinet : une exigence de qualité…, *Cah. Nutr. Diététique*, 2009, **44**, 294–301.
34 M. Baudu, G. Guibaud, D. Raveau and P. Lafrance, Prévision de l'adsorption de molécules organiques en solution aqueuse en fonctions de quelques caractéristiques physico-chimiques de charbons actifs, *Water Qual. Res. J.*, 2001, **36**, 631–657.
35 N. Barka, M. Abdennouri, A. Boussaoud and M. E. Makhfouk, Biosorption characteristics of Cadmium(II) onto Scolymus hispanicus L. as low-cost natural biosorbent, *Desalination*, 2010, **258**, 66–71.
36 K. S. Baidya and U. Kumar, Adsorption of brilliant green dye from aqueous solution onto chemically modified areca nut husk, *S. Afr. J. Chem. Eng.*, 2021, **35**, 33–43.
37 T. A. Saleh, in *Surface Science of Adsorbents and Nanoadsorbents*, ed. T. A. Saleh, Elsevier, 2022, vol. 34, pp. 39–64.
38 H. Esmaeili and R. Foroutan, Adsorptive Behavior of Methylene Blue onto Sawdust of Sour Lemon, Date Palm, and Eucalyptus as Agricultural Wastes, *J. Dispersion Sci. Technol.*, 2019, **40**, 990–999.
39 K. Naseem, in *Sodium Alginate-Based Nanomaterials for Wastewater Treatment*, ed. A. Ahmad, I. Ahmad, T. Kamal, A. M. Asiri and S. Tabassum, Elsevier, 2023, pp. 137–159.
40 L. Mishra, K. K. Paul and S. Jena, Adsorption Isotherm, Kinetics and Optimization Study by Box Behnken Design on Removal of Phenol from Coke Wastewater Using Banana Peel (Musa sp.) Biosorbent, *Theor. Found. Chem. Eng.*, 2022, **56**, 1189–1203.
41 H. A. Gzar, K. M. Kseer and M. J. Nasir, Kinetics and Isotherms of a Green Method for the Sorption of Metal Ions from Aqueous Solution, *IOP Conf. Ser.: Mater. Sci. Eng.*, 2020, **888**, 012077.
42 Y. S. Ho and G. McKay, Pseudo-second order model for sorption processes, *Process Biochem.*, 1999, **34**, 451–465.
43 K. Vijayaraghavan and Y.-S. Yun, Bacterial biosorbents and biosorption, *Biotechnol. Adv.*, 2008, **26**, 266–291.
44 L. Wang and A. Wang, Adsorption properties of Congo Red from aqueous solution onto surfactant-modified montmorillonite, *J. Hazard. Mater.*, 2008, **160**, 173–180.
45 V. M. Bhandari and V. V. Ranade, in *Industrial Wastewater Treatment, Recycling and Reuse*, ed. V. V. Ranade and V. M. Bhandari, Butterworth-Heinemann, Oxford, 2014, pp. 81–140.
46 G. Annadurai, R.-S. Juang and D.-J. Lee, Use of cellulose-based wastes for adsorption of dyes from aqueous solutions, *J. Hazard. Mater.*, 2002, **92**, 263–274.
47 K. G. Bhattacharyya and A. Sharma, Kinetics and thermodynamics of Methylene Blue adsorption on Neem (Azadirachta indica) leaf powder, *Dyes Pigm.*, 2005, **65**, 51–59.
48 S. Wang, Y. Boyjoo and A. Choueib, A comparative study of dye removal using fly ash treated by different methods, *Chemosphere*, 2005, **60**, 1401–1407.
49 W. T. Tsai, J. M. Yang, C. W. Lai, Y. H. Cheng, C. C. Lin and C. W. Yeh, Characterization and adsorption properties of

eggshells and eggshell membrane, *Bioresour. Technol.*, 2006, **97**, 488–493.

50 Y. Bulut and H. Aydın, A kinetics and thermodynamics study of methylene blue adsorption on wheat shells, *Desalination*, 2006, **194**, 259–267.

51 S. M. Anisuzzaman, C. G. Joseph, D. Krishnaiah, A. Bono and L. C. Ooi, Parametric and adsorption kinetic studies of methylene blue removal from simulated textile water using durian (Durio zibethinus murray) skin, *Water Sci. Technol.*, 2015, **72**, 896–907.

52 W. Hassan, U. Farooq, M. Ahmad, M. Athar and M. A. Khan, Potential biosorbent, Haloxylon recurvum plant stems, for the removal of methylene blue dye, *Arab. J. Chem.*, 2017, **10**, S1512–S1522.

53 R. Fiaz, M. Hafeez and R. Mahmood, Ficcus palmata leaves as a low-cost biosorbent for methylene blue: Thermodynamic and kinetic studies, *Water Environ. Res.*, 2019, **91**, 689–699.

54 N. T. Dinh, L. N. H. Vo, N. T. T. Tran, T. D. Phan and D. B. Nguyen, Enhancing the removal efficiency of methylene blue in water by fly ash via a modified adsorbent with alkaline thermal hydrolysis treatment, *RSC Adv.*, 2021, **11**, 20292–20302.

55 S. A. Mousavi, D. Shahbazi, A. Mahmoudi and P. Darvishi, Methylene blue removal using prepared activated carbon from grape wood wastes: adsorption process analysis and modeling, *Water Qual. Res. J.*, 2021, **57**, 1–19.

56 S. Radoor, J. Karayil, A. Jayakumar, J. Parameswaranpillai, J. Lee and S. Siengchin, Ecofriendly and low-cost bio adsorbent for efficient removal of methylene blue from aqueous solution, *Sci. Rep.*, 2022, **12**, 20580.

57 T. Juzsakova, A. D. Salman, T. A. Abdullah, R. T. Rasheed, B. Zsirka, R. R. Al-Shaikhly, B. Sluser and I. Cretescu, Removal of Methylene Blue from Aqueous Solution by Mixture of Reused Silica Gel Desiccant and Natural Sand or Eggshell Waste, *Materials*, 2023, **16**(4), 1618.

58 C. Bouyahia, M. Rahmani, M. Bensemlali, S. E. Hajjaji, M. Slaoui, I. Bencheikh, K. Azoulay and N. Labjar, Influence of extraction techniques on the adsorption capacity of methylene blue on sawdust: Optimization by full factorial design, *Mater. Sci. Energy Technol.*, 2023, **6**, 114–123.